

Research Article

Thermal Stability and Rheological Behaviors of High-Density Polyethylene/Fullerene Nanocomposites

Liping Zhao,^{1,2} Ping'an Song,³ Zhenhu Cao,^{1,2} Zhengping Fang,^{1,2}
and Zhenghong Guo¹

¹Laboratory of Polymer Materials and Engineering, Ningbo Institute of Technology, Zhejiang University, Ningbo 315100, China

²MOE Key Laboratory of Macromolecular Synthesis and Functionalization, Zhejiang University, Hangzhou 310027, China

³Department of Materials, College of Engineering, Zhejiang Agriculture & Forest University, Hangzhou 300311, China

Correspondence should be addressed to Zhenghong Guo, guozhenghong@nit.zju.edu.cn

Received 3 June 2011; Accepted 20 October 2011

Academic Editor: Steve Acquah

Copyright © 2012 Liping Zhao et al. This is an open access article distributed under the Creative Commons Attribution License, which permits unrestricted use, distribution, and reproduction in any medium, provided the original work is properly cited.

High-density polyethylene/fullerene (HDPE/C₆₀) nanocomposites with the C₆₀ loading that varied from 0.5 to 5.0% by weight were prepared via melt compounding. Thermogravimetric analysis (TGA) and differential scanning calorimetry (DSC) results showed that the presence of C₆₀ could remarkably enhance the thermal properties of HDPE. A very low C₆₀ loading (0.5 wt%) increased the onset degradation temperature from 389°C to 459°C and decreased the heat release from 3176 J/g to 1490 J/g. The larger the loading level of C₆₀, the better the thermal stability of HDPE/C₆₀ nanocomposites. Rheological investigation results showed that the free radical trapping effect of C₆₀ was responsible for the improved thermal stability of HDPE.

1. Introduction

Soon after the discovery of buckminsterfullerene, C₆₀, it was able to be produced in bulk quantities, which inspired scientists worldwide to explore its fascinating chemistry, and it has now become the most intensely researched single molecule in modern science [1–3]. A significant aspect of the C₆₀ chemistry is its high reactivity towards free radicals, and C₆₀ has 30 carbon-carbon double bonds which can trap more than 34 free radicals; thus it is known as a radical sponge [4]. The free radical reaction of C₆₀ with various compounds has been extensively studied [4–7].

Since the thermal degradation of polymers is a free radical chain reaction, the presence of C₆₀ in polymer may trap the free radicals produced during the degradation process. These suggest the possible use of fullerene as an effective radical scavenger in chain reactions during thermal degradation. It has been reported that 2 wt% fullerene (C₆₀) could increase the onset degradation temperature (T_{onset}) and the maximum degradation temperature (T_{max}) of PP by 20 and 62°C, respectively [8, 9]. The presence of C₆₀ could delay the thermal oxidation and improve the thermal

stability of PP, which could be attributed to the high reactivity of C₆₀ towards free radicals.

The present paper mainly focused on studying the influence of C₆₀ on the thermal degradation behavior and rheological properties of high-density polyethylene. Concerning that the thermal degradation of polyethylene is done also via a free radical chain scission process as PP, C₆₀ is expected to have positive effect on improving the thermal stability of PE.

2. Materials and Methods

2.1. Materials. High-density Polyethylene (HDPE, 5000 S, MFR = 0.9 g/10 min) was purchased from Yangzi Petrochemical Co., Ltd, and C₆₀ (purity: >99%) was bought from Henan Puyang Co., Ltd.

2.2. Preparation of HDPE/C₆₀ Nanocomposites. HDPE/C₆₀ nanocomposites were prepared via melt compounding at 180°C in a ThermoHaake rheomixer with a rotor speed of 60 rpm for 8 min. Nanocomposites containing 0.5 wt%, 1.0 wt%, 2.5 wt%, and 5.0 wt% C₆₀ were designated as C₆₀-0.5%, C₆₀-1.0%, C₆₀-2.5%, and C₆₀-5.0%.

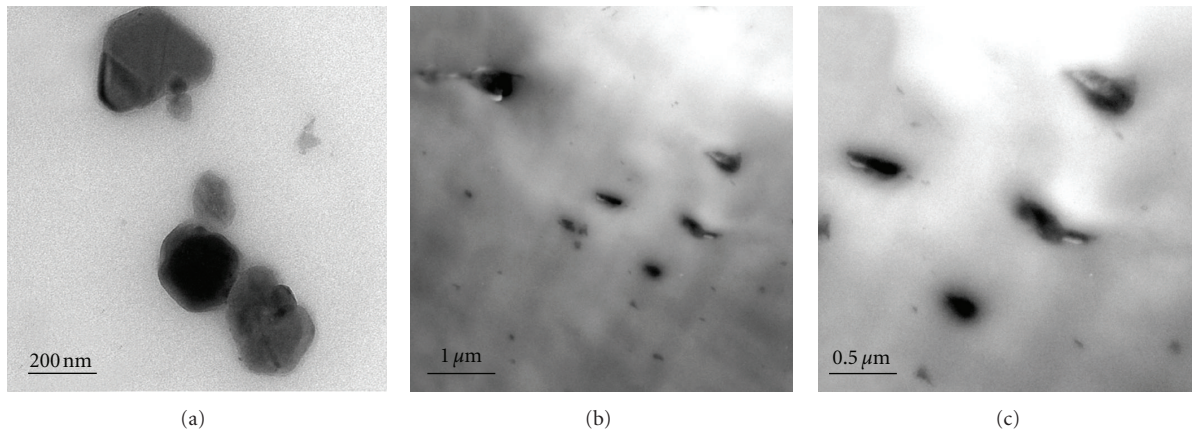


FIGURE 1: TEM microphotographs for pristine C_{60} (a) and C_{60} -5.0% (b) and (c).

2.3. Measurements and Characterization. Thermogravimetric analysis (TGA) was performed on a STA 409 PC thermal analyzer at a heating rate of $20^{\circ}\text{C}/\text{min}$ in air atmosphere and N_2 atmosphere, with a scanning range from 30 to 700°C , and each specimen was examined in triplicate.

The rheological properties of HDPE and its nanocomposites were conducted on a controlled strain rheometer (Haake MARS) in air environment. The samples were pressed at 180°C under 15 MPa to get the disklike specimens with 25 mm in diameter and 1.2 mm in thickness. The isothermal dynamic frequency sweeps were performed under the condition of the frequency range, strain amplitude, and temperature being $100\text{--}0.01\text{ rads}^{-1}$ with the strain of 1% at 180°C and 300°C , respectively. Temperature scanning test was performed in the range from 180 to 300°C with the 1% strain and a fixed frequency at 1 rads^{-1} .

The dispersion of C_{60} in the HDPE matrix was observed by transmission electron microscopy (TEM, JEM-1200EX).

3. Results and Discussion

3.1. Dispersion of C_{60} in HDPE Matrix. The diameter of the spherical C_{60} molecule is 0.71 nm , and its crystal size differs with different methods of fabrication [9]. Figure 1 shows the TEM images for pure C_{60} and C_{60} -5%. The size of C_{60} crystals used in this work from Figure 1(a) is from 70 to 200 nm . From Figure 1(c), it is shown that many of C_{60} crystallites in the HDPE matrix were shaped in ellipsoidal, rodlike. This phenomenon may be caused by the strong shear force during blending. The shear force could destroy the primary stack of C_{60} crystallites and these crystallites rearrange to different type. In the HDPE matrix, C_{60} crystallites aggregates and does not disperse well through melt blending, as observed from Figure 1(b). The size of some C_{60} domains in nanocomposites is about 500 nm or even large.

3.2. Thermal Properties of HDPE/ C_{60} Nanocomposites. The thermal stability of HDPE and HDPE/ C_{60} nanocomposites was tested by TGA, and their TG and DTG curves in nitrogen

TABLE 1: Detailed data obtained from TGA tests for HDPE and HDPE/ C_{60} nanocomposites in nitrogen.

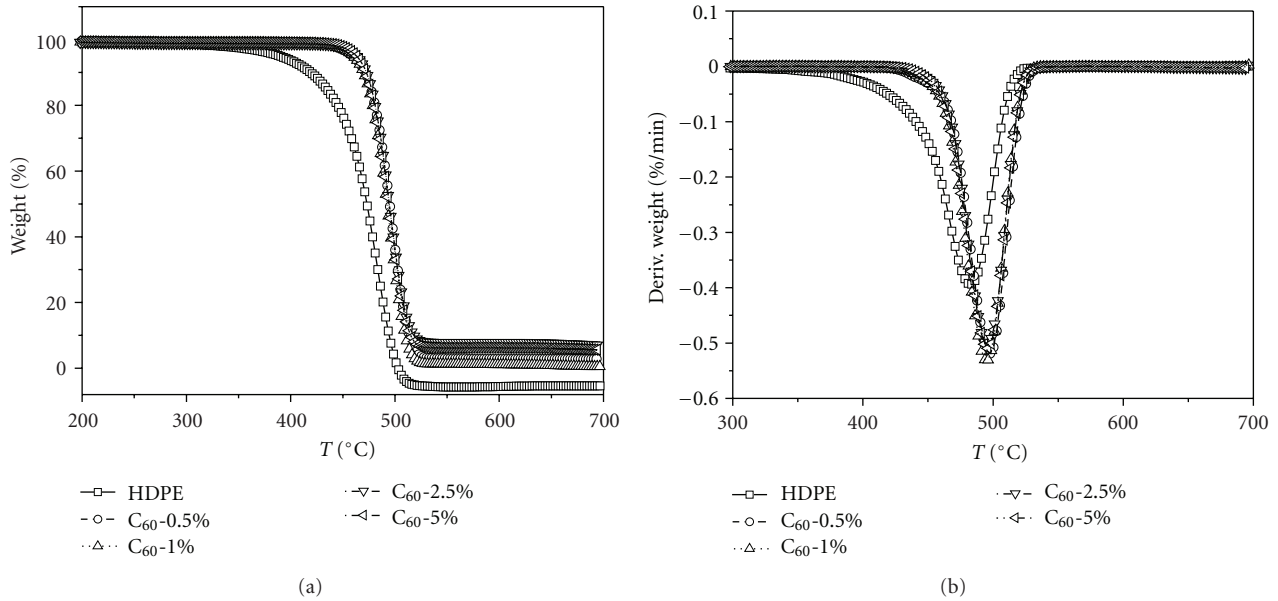
| Sample | $T_{\text{onset}} (^{\circ}\text{C})$ | $T_{\text{max}} (^{\circ}\text{C})$ |
|----------------|---------------------------------------|-------------------------------------|
| HDPE | 389 | 483 |
| C_{60} -0.5% | 459 | 497 |
| C_{60} -1.0% | 460 | 496 |
| C_{60} -2.5% | 462 | 496 |
| C_{60} -5.0% | 463 | 495 |

atmosphere are shown in Figure 2, with detailed data listed in Table 1. At the initial stage of degradation (before 400°C), C_{60} reacts easily with low-molecular-weight alkyl radicals with formation of remarkable persistent products $\text{Rn}C_{60}$ (where $n = 1, 2, 3, \dots$) [10, 11], which caused that the decomposition of HDPE/ C_{60} nanocomposites is slower than pure HDPE. The onset thermal decomposition temperature (T_{onset}) of HDPE is noticeably increased with the addition of C_{60} . For example, the T_{onset} of C_{60} -0.5% is 459°C , about 70°C higher than pure HDPE. With increasing C_{60} content, the onset temperature of HDPE/ C_{60} nanocomposites changes slightly. From DTG curves, the maximum decomposition temperature (T_{max}) is obtained, with T_{max} 497°C for C_{60} -0.5%, about 14°C higher than pure HDPE.

Figures 3 and 4 present the TG and DSC curves for HDPE and its composites in air atmosphere, with detailed data given in Table 2. In air atmosphere, the presence of oxygen could enhance the thermal oxidation decomposition of HDPE nanocomposites remarkably. HDPE experiences a rapid thermal oxidation decomposition accompanied by hydrogen abstraction [12]. The (T_{onset}) of HDPE is about 323°C , and two-step decomposition processes are observed at around 398°C and 456°C (see Table 2). The first step decomposition is the oxidation of HDPE [13]. The second step may be the decomposition of oxidation products formed by the oxidation of HDPE. C_{60} , as the radical sponge, could capture the free radicals produced during the degradation process. Obviously, the presence of C_{60} delays the oxidation degradation of parent polymer and the first-step T_{max} disappears, and the T_{onset} of the nanocomposites noticeably

TABLE 2: Detailed data obtained from TGA and DSC tests for HDPE and HDPE/C₆₀ nanocomposites in air.

| Sample | T_{onset} (°C) | Data from TGA | | T_{max} | Data from DSC ΔH_d (J/g) |
|-----------------------|-------------------------|---------------|---------|------------------|----------------------------------|
| | | Stage 1 | Stage 2 | | |
| HDPE | 323 | 398 | 456 | | 3176 |
| C ₆₀ -0.5% | 361 | — | 451 | | 1490 |
| C ₆₀ -1.0% | 387 | — | 444 | | 1521 |
| C ₆₀ -2.5% | 431 | — | 461 | | 842 |
| C ₆₀ -5.0% | 416 | — | 448 | | 1892 |

FIGURE 2: TG (a) and DTG (b) curves for pristine HDPE and HDPE/C₆₀ nanocomposites in nitrogen.

increase with the increase of C₆₀ content. As for C₆₀-2.5%, its T_{onset} is around 431°C, 108°C higher than pure HDPE, which indicates that the presence of C₆₀ slows down the thermal oxidation decomposition of HDPE remarkably. However, when the contents of C₆₀ in the matrix exceed 2.5 wt%, the T_{onset} of the nanocomposites decreases with the content of C₆₀. At high loading (as for C₆₀-5.0%), C₆₀ may tend to attract each other, which causes the agglomeration (as shown in Figure 1) instead of trapping the alkyl fragments radicals bringing down the thermal stability of HDPE/C₆₀ nanocomposites.

The difference in thermal behavior between air and nitrogen atmospheres indicates that the presence of oxygen could speed up the thermal oxidation decomposition of HDPE nanocomposites remarkably. The oxygen and alkyl fragment radicals trapped by C₆₀ in nanocomposites during the thermal decomposition are competitive.

DSC measurements could provide the heat enthalpy of thermal degradation during the decomposition process of materials. Figure 4 presents the DSC curves of HDPE/C₆₀ nanocomposites in air atmosphere. In air atmosphere, HDPE/C₆₀ nanocomposites experiences rapid exothermal oxidation decomposition at high temperature. The enthalpy

(ΔH_d) is an important parameter since it could quantify the heat evolution produce in the process of oxidation decomposition. The enthalpies of the nanocomposites are greatly reduced from 3176 J/g for HDPE to 1490 J/g for C₆₀-0.5%, indicating that the nanocomposites release much less heat in the process of oxidation dehydrogenation and this phenomenon is favorable to flame retarded polymer materials.

3.3. Mechanism for the Thermal Stability of HDPE/C₆₀ Nanocomposites. In order to clarify the mechanism for C₆₀ improving the thermal stability of HDPE, the rheological measurements were introduced to investigate the viscoelastic behaviors of the nanocomposites. For investigating the viscoelastic behavior of the nanocomposites in the heating process, temperature scanning measurements were performed. Figure 5 presents the curves of temperature dependence of complex viscosity (η^*) for HDPE and its nanocomposites. Clearly, with the increase of temperature, the complex viscosity (η^*) of nanocomposites decreases, and then increases sharply. The critical temperature is defined as T_c , at which η^* starts to increase or crosslink reaction occurs. The easier movement of polymer chains during heating, or

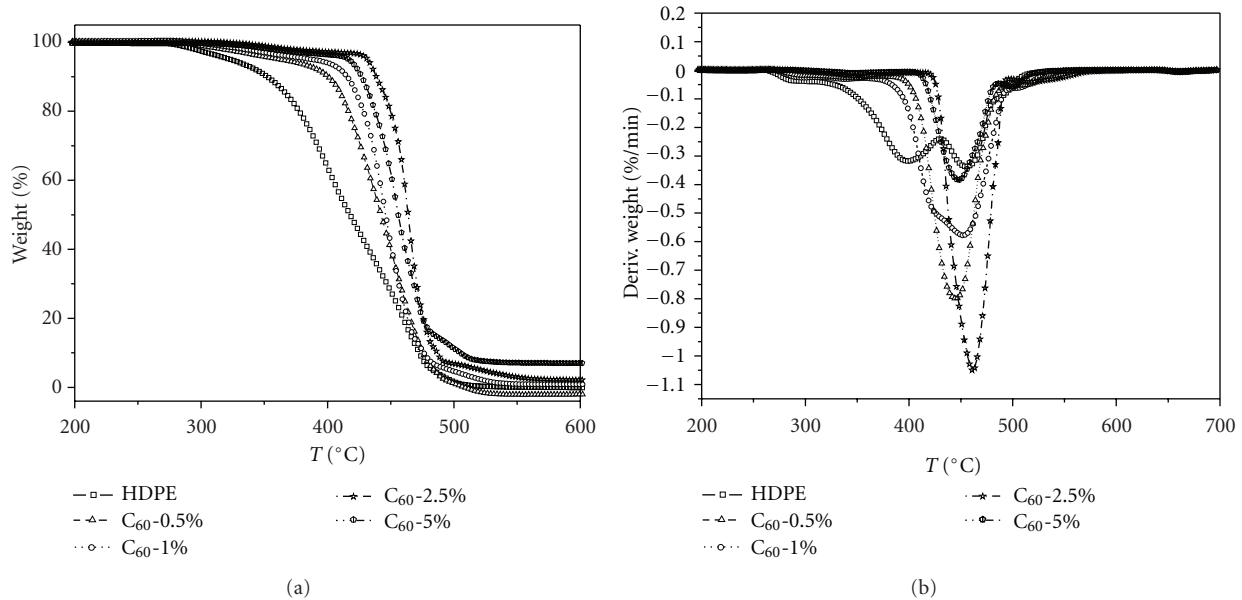


FIGURE 3: TG (a) and DTG (b) curves for pristine HDPE and nanocomposites in air.

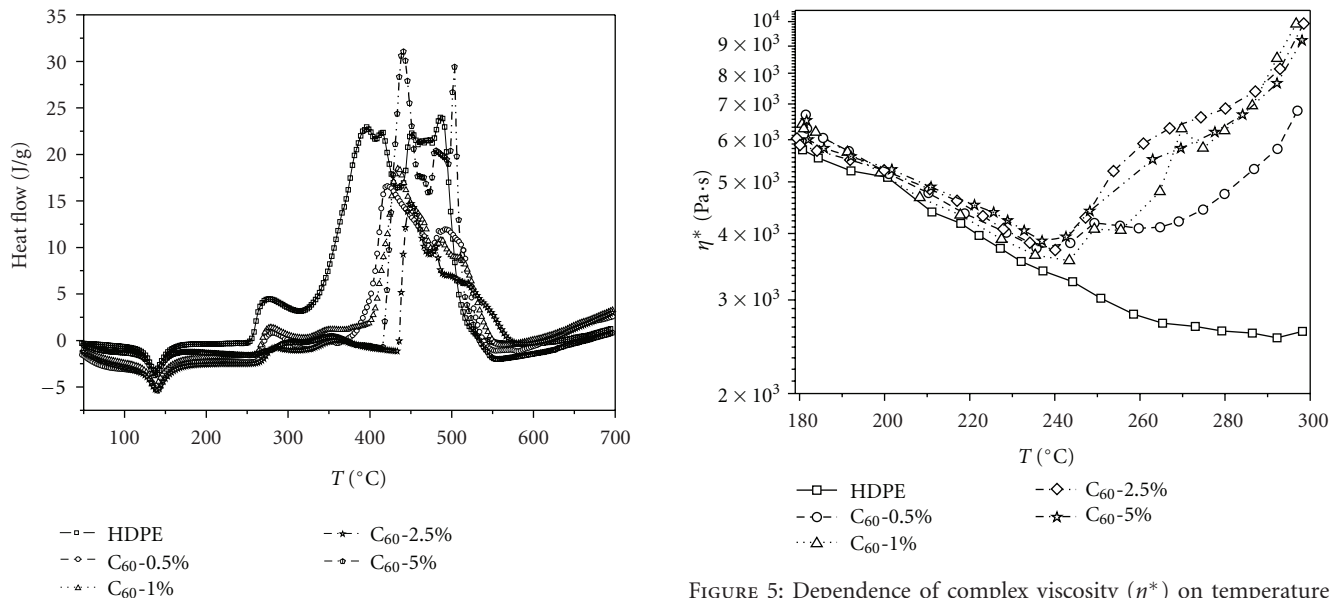


FIGURE 4: DSC curves for HDPE and HDPE/C₆₀ nanocomposites.

the occurrence of degradation of polymer can cause the decrease of η^* . The increase of η^* is due to the occurrence of an oxidation crosslink or the oxidation crosslink reaction overwhelming the polymer decomposition. In the case of pure HDPE, it gives a T_c of 285°C. For HDPE/C₆₀ nanocomposites, their T_c is about 45°C lower than that of HDPE, implying that another kind of crosslink reaction occurred in the process of heating for HDPE/C₆₀ systems, which speeds up the crosslink reaction whether before or after oxidation crosslinking takes place.

FIGURE 5: Dependence of complex viscosity (η^*) on temperature for HDPE and HDPE/C₆₀ nanocomposites.

The viscoelastic behaviors of the nanocomposites at 180°C were studied and those of parent polymer, HDPE, were also used as a comparison. Figures 6 and 7 show the storage moduli (G') and complex viscosity (η^*) as a function of frequency (ω) of HDPE and its nanocomposites. Some researchers have found that both G' and η^* have much larger values than those of parent polymers in the low ω regime for the nanocomposites containing CNTs [14–17] or clay [18, 19], suggesting that the presence of CNTs or clay affects the relaxation and motion of polymer chains due to their spatial geometry. Most authors attribute these viscoelastic behaviors to the formation of CNT or clay networks in the

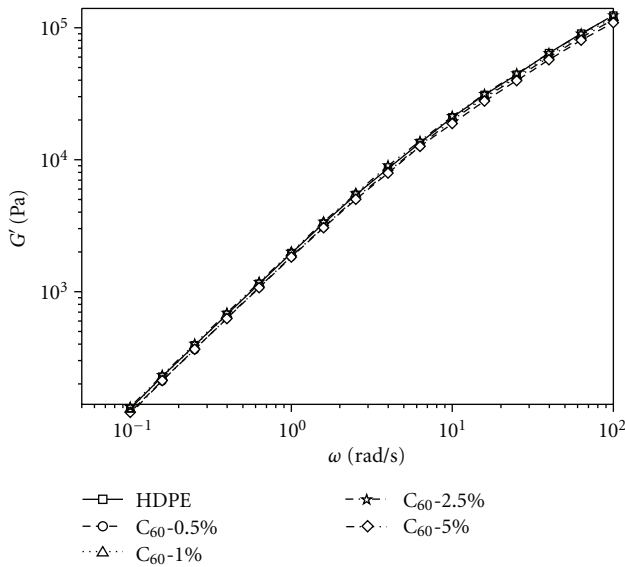


FIGURE 6: Plots of storage moduli (G') versus shifted frequency for consecutive small amplitude oscillatory shear sweeps performed at 180°C .

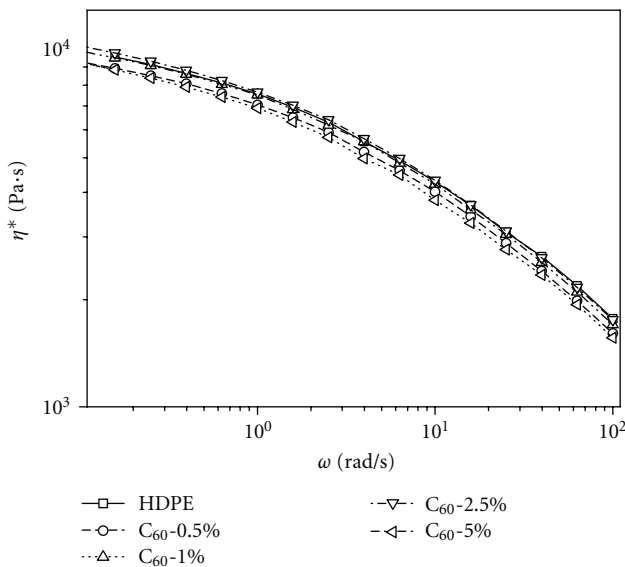


FIGURE 7: Plots of complex viscosity versus shifted frequency for consecutive small amplitude oscillatory shear sweeps performed at 180°C .

polymer matrix. However, in the high ω region, the addition of CNTs and clay does not significantly affect the G' or η^* of polymers. Unlike CNTs and clay, whether in the low ω region or high ω region, not much obvious difference in G' and η^* is observed for the HDPE/ C_{60} nanocomposites with various C_{60} contents. The oxidation degradation of HDPE does not occur at 180°C (as shown in Figure 3 and Table 2). And not enough free radicals react with C_{60} . Therefore, the incorporation of C_{60} does not affect the movement and relaxation of polymer chain segments remarkably.

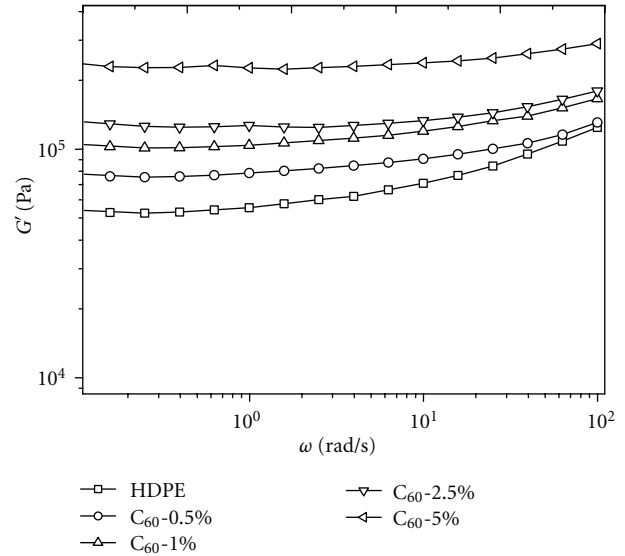


FIGURE 8: Plots of storage modulus versus shifted frequency for consecutive small amplitude oscillatory shear sweeps performed at 300°C .

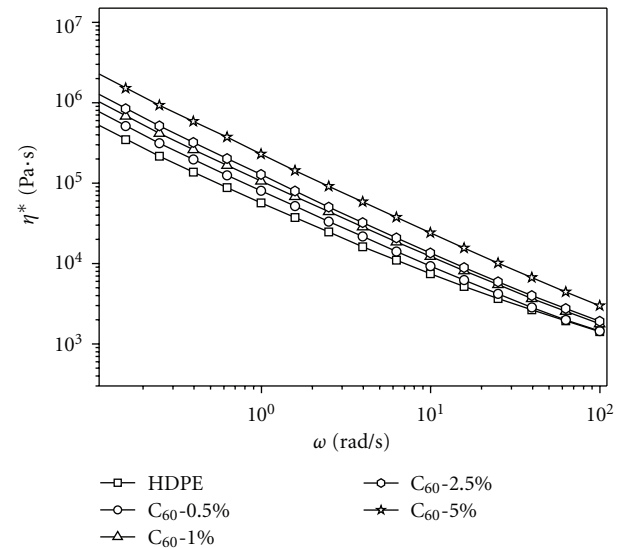


FIGURE 9: Plots of complex viscosity versus shifted frequency for consecutive small amplitude oscillatory shear sweeps performed at 300°C .

The viscoelastic behaviors of the nanocomposites at 300°C after dynamic temperature scanning measurements were also studied. Figures 8 and 9 show the storage moduli (G') and complex viscosity (η^*) as a function of frequency (ω) of HDPE and its nanocomposites at 300°C . The increase of complex viscosity with C_{60} content is concomitant with the increase of the storage moduli. The storage moduli for the nanocomposites show a monotonic increase at all frequencies with increasing C_{60} content. The G' versus frequency curve for the nanocomposites appears to be approaching a plateau at low frequencies. It has been proposed that this “plateau” effect is derived from interconnected structures of

isometric fillers that result in an apparent yield stress which is manifest by a plateau in either G' or η^* versus frequency plots [20, 21]. Exposed at 300°C for a long time, many alkyl radicals appear, coupled with the interfacial interactions between free radicals and C_{60} . The restraint for the move and relaxation of polymer chains increased G' and η^* , which is the evidence for the presence of a chemical reaction between the HDPE matrix and C_{60} .

4. Conclusion

The presence of C_{60} could enhance the thermal stability of HDPE. A very low C_{60} loading (0.5 wt%) increases the T_{onset} from 389°C to 459°C and decreases the heat release from 3176 J/g to 1490 J/g. The free radical trapping effect of C_{60} is responsible for the improved thermal stability of HDPE. Thus, C_{60} is expected to be an efficient thermal stabilizer to the polymer materials that degraded with a free radical chain scission process.

Acknowledgment

This work was financially supported by the National Natural Science Foundation of China (no. 51073140).

References

- [1] D. E. H. Jones, "The academic sphere," *Nature*, vol. 381, no. 6581, pp. 381–384, 1996.
- [2] R. Taylor and D. R. M. Walton, "The chemistry of fullerenes," *Nature*, vol. 363, no. 24, pp. 685–693, 1993.
- [3] F. Diederich and C. Thilgen, "Covalent fullerene chemistry," *Science*, vol. 271, no. 5247, pp. 317–323, 1996.
- [4] P. J. Krusic, E. Wasserman, P. N. Keizer, J. R. Morton, and K. F. Preston, "Radical reactions of C_{60} ," *Science*, vol. 254, no. 5035, pp. 1183–1185, 1991.
- [5] L. B. Gan, S. H. Huang, X. Zhang et al., "Fullerenes as a tert-butylperoxy radical trap, metal catalyzed reaction of tert-butyl hydroperoxide with fullerenes, and formation of the first fullerene mixed peroxides $C_{60}(O)(OO^tBU)_4$ and $C_{70}(OO^tBU)_{10}$," *Journal of the American Chemical Society*, vol. 124, no. 45, pp. 13384–13385, 2002.
- [6] B. Z. Tang, S. M. Leung, H. Peng, N. T. Yu, and K. C. Su, "Direct fullerenation of polycarbonate via simple polymer reactions," *Macromolecules*, vol. 30, no. 10, pp. 2848–2852, 1997.
- [7] T. Cao and S. E. Webber, "Free radical copolymerization of styrene and C_{60} ," *Macromolecules*, vol. 29, no. 11, pp. 3826–3830, 1996.
- [8] Z. P. Fang, P. A. Song, L. F. Tong, and Z. H. Guo, "Thermal degradation and flame retardancy of polypropylene/ C_{60} nanocomposites," *Thermochimica Acta*, vol. 473, no. 1-2, pp. 106–108, 2008.
- [9] P. A. Song, Z. P. Fang, Y. Zhu, and L. Tong, " C_{60} reduces the flammability of polypropylene nanocomposites by *in situ* forming a gelled-ball network," *Nanotechnology*, vol. 19, no. 22, Article ID 225707, 2008.
- [10] P. J. Krusic, E. Wasserman, B. A. Parkinson et al., "Electron spin resonance study of the radical reactivity of C_{60} ," *Journal of the American Chemical Society*, vol. 113, no. 16, pp. 6274–6275, 1991.
- [11] J. R. Morton, K. F. Preston, P. J. Krusic, S. A. Hill, and E. Wasserman, "The dimerization of RC_{60} radicals," *Journal of the American Chemical Society*, vol. 114, no. 13, pp. 5454–5455, 1992.
- [12] M. Zanetti, G. Camino, P. Reichert, and R. Mulhaupt, "Thermal behaviour of poly(propylene) layered silicate nanocomposites," *Macromolecular Rapid Communications*, vol. 22, no. 3, pp. 176–180, 2001.
- [13] G. Wu, Y. Song, Q. Zheng, M. Du, and P. Zhang, "Dynamic rheological properties for HDPE/CB composite melts," *Journal of Applied Polymer Science*, vol. 88, no. 9, pp. 2160–2167, 2003.
- [14] T. Kashiwagi, E. Grulke, J. Hilding, R. Harris, W. Awad, and J. Douglas, "Thermal degradation and flammability properties of poly(propylene)/carbon nanotube composites," *Macromolecular Rapid Communications*, vol. 23, no. 13, pp. 761–765, 2002.
- [15] T. Kashiwagi, F. Du, K. I. Winey et al., "Flammability properties of polymer nanocomposites with single-walled carbon nanotubes: effects of nanotube dispersion and concentration," *Polymer*, vol. 46, no. 2, pp. 471–481, 2005.
- [16] T. Kashiwagi, F. Du, J. F. Douglas, K. I. Winey, R. H. Harris, and J. R. Shields, "Nanoparticle networks reduce the flammability of polymer nanocomposites," *Nature Materials*, vol. 4, no. 12, pp. 928–933, 2005.
- [17] S. B. Kharchenko, J. F. Douglas, J. Obrzut, E. A. Grulke, and K. B. Migler, "Flow-induced properties of nanotube-filled polymer materials," *Nature Materials*, vol. 3, no. 8, pp. 564–568, 2004.
- [18] M. A. Trece and J. P. Oberhauser, "Soft glassy dynamics in polypropylene-clay nanocomposites," *Macromolecules*, vol. 40, no. 3, pp. 571–582, 2007.
- [19] C. O. Rohlmann, M. D. Failla, and L. M. Quinzani, "Linear viscoelasticity and structure of polypropylene-montmorillonite nanocomposites," *Polymer*, vol. 47, no. 22, pp. 7795–7804, 2006.
- [20] P. Potschke, M. Abdel-Goad, I. Alig, S. Dudkin, and D. Lellinger, "Rheological and dielectrical characterization of melt mixed polycarbonate-multiwalled carbon nanotube composites," *Polymer*, vol. 45, no. 26, pp. 8863–8870, 2004.
- [21] L. A. Utracki, "Flow and flow orientation of composites containing anisometric particles," *Polymer Composites*, vol. 7, no. 5, pp. 274–282, 1986.



Hindawi

Submit your manuscripts at
<http://www.hindawi.com>

